Theoretical Modelling of High-Resolution X-Ray Absorption Spectra at Uranium M4 Edge

Kolorenc, J.; Kvashnina, K.;

Originally published:

May 2018

MRS Bulletin 3(2018)53, 3143-3148

DOI: https://doi.org/10.1557/adv.2018.470

MRS Advances

Theoretical Modelling of High-Resolution X-Ray Absorption Spectra at Uranium M_4 Edge

Journal:	*MRS Advances*
Manuscript ID	Draft
Manuscript Type:	Regular Article
Date Submitted by the Author:	n/a
Complete List of Authors:	Kolorenc, Jindrich; Institute of Physics, Czech Academy of Sciences, Kvashnina, Kristina; European Synchrotron Radiation Facility (ESRF),
Keywords:	spectroscopy, modeling, actinide, oxide, electronic structure

MRS Advances

Theoretical Modelling of High-Resolution X-Ray Absorption Spectra at Uranium M_4 Edge

Jindřich Kolorenč[1] and Kristina O. Kvashnina[2,3]

[1]*Institute of Physics, Czech Academy of Sciences, Na Slovance 2, 182 21 Praha, Czech Republic*

[2]*Institute of Resource Ecology, Helmholtz-Zentrum Dresden-Rossendorf, 01314 Dresden, Germany*

[3]*European Synchrotron Radiation Facility, 71 Avenue des Martyrs, 38000 Grenoble, France*

We investigate the origin of satellite features that appear in the high-resolution x-ray absorption spectra measured at the uranium M_4 edge in compounds where the uranium atoms are in the U^{6+} oxidation state. We employ a material-specific Anderson impurity model derived from the electronic structure obtained by the density-functional theory.

INTRODUCTION

The resolution of the x-ray absorption spectroscopy is fundamentally limited by the life-time broadening of the core hole created in the absorption event. For the actinide M edges (3d → 5f transitions), this broadening is large due to a short life time of the deep 3d hole (∼0.7 eV). However, when the absorption is detected by monitoring a particular core-to-core process of filling the created hole (the 4f → 3d transition in the case of the actinide M edge), the broadening is reduced and it is determined by a considerably longer life time of the shallower 4f hole (∼0.3 eV) [1]. This method is referred to as the high-energy-resolution fluorescence-detected x-ray absorption spectroscopy (HERFD-XAS) in the literature [2]. The spectra recorded in this way do not exactly coincide with the conventional x-ray absorption: XAS involves only one photon and can be calculated from the Fermi golden rule, whereas HERFD-XAS involves two photons and thus should be modelled by the Kramers–Heisenberg formula. Nevertheless, the Kramers–Heisenberg formula simplifies to an expression very similar to the conventional XAS formula in certain cases. One set of such simplifying assumptions was recently discussed in the context of the resonant x-ray emission spectroscopy (RXES) at the L-edge of lanthanides [3]: If (i) the shape of the core orbitals can be neglected so that the core-valence Coulomb interaction is fully determined by just one Slater integral, (ii)

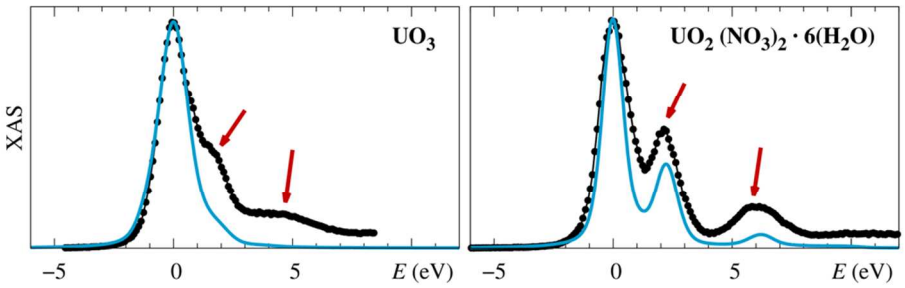

Figure 1. The experimental HERFD spectra at the uranium M_4 edge of UO_3 and uranyl nitrate (black dots) are compared to $j = 5/2$ component of the f-electron density of states computed in the local-density approximation (blue line). The LDA density of states is artificially broadened with a Voight profile to approximately match the width of the main line. The broadening parameters are the same for all theoretical spectra shown in this paper. The satellite features discussed in the text are indicated with arrows.

if this core-valence Slater integral is the same in the intermediate state (3d hole) and in the final state (4f hole), and (iii) if the detector registers all polarizations of the emitted photon equally, then the HERFD-XAS essentially coincides with the conventional XAS, only the life-time broadening is described by a function that slightly differs from the Lorentzian. The calculations presented in this paper are performed under these assumptions.

We investigate absorption at the uranium M_4 edge ($3d_{3/2} \rightarrow 5f_{5/2}$) in compounds where the uranium atoms are in the U^{6+} oxidation states. The compounds in question are α-UO_3 and uranyl nitrate $UO_2(NO_3)_2 \cdot 6(H_2O)$. The experimental spectra are shown in Figure 1. Two extra features are found above the main absorption line in both compounds: two shoulders in UO_3 and two well defined satellites in uranyl nitrate. Very similar spectrum to uranyl nitrate is measured also for other compounds containing the $(UO_2)^{2+}$ molecular ion, such as uranyl acetylacetonate and torbentite [4]. It suggests that this spectral shape is essentially determined by this uranyl-type of ion.

COMPUTATIONAL METHOD

The absorption spectra are computed by exact diagonalization of a material-specific Anderson impurity model that represents the uranium 5f shell and its environment. To construct the model, we employ the method previously implemented for LDA+DMFT calculations of actinide dioxides [5]. First, the band structure is computed in the local-density approximation (LDA) with the aid of the WIEN2K code [6] and then the relevant bands are represented by a tight-binding hamiltonian in the basis of the corresponding Wannier functions [7,8]. The local electronic structure around one shell of 5f Wannier functions is subsequently mapped to a non-interacting impurity model. The construction of the impurity model suitable for calculation of core-level spectra is finished by introducing a spherically symmetric Coulomb vertex acting among the 5f orbitals (this vertex is parametrized by four Slater integrals $U = F_0 = 6.5$ eV, $F_2 = 8.1$ eV, $F_4 = 5.4$ eV, $F_6 = 4.0$ eV) and by adding the appropriate core orbitals and the corresponding core-valence Coulomb interaction parametrized by a single Slater integral U_{cv}. The valence Coulomb parameters are chosen the same as in the earlier study of actinide dioxides [5], the core-valence Coulomb parameter is taken equal to the valence Slater integral, $U_{cv} = U = 6.5$ eV, for simplicity.

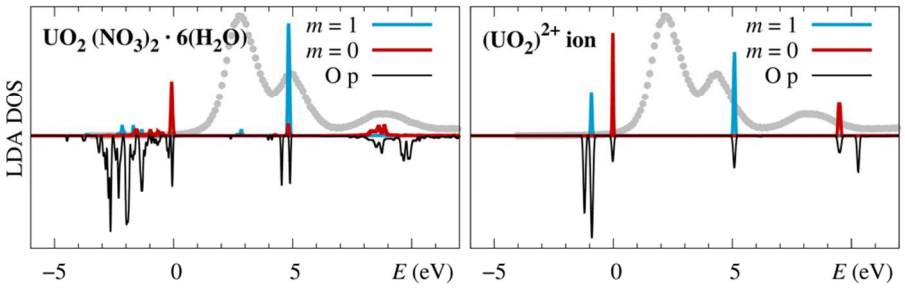

Figure 2. The origin of the satellite features in uranyl nitrate is illustrated using similarity to a lone $(UO_2)^{2+}$ ion. The LDA density of states (with the spin-orbital coupling switched off) is projected onto uranium 5f functions with $|m = 1\rangle$ and $|m = 0\rangle$ character, and onto 2p functions of the two nearest-neighbor oxygen atoms.

Majority of the calculations presented in this paper are performed for the experimental crystal structures. The α phase of UO_3 has the space group $P\bar{3}m1$, the uranium atoms are located in 1a positions and the oxygen atoms occupy 2d ($z = 0.17$) and 1b positions. The uranyl nitrate crystallizes in the low-symmetry $Cmc2_1$ structure. It has two formula units (58 atoms) in the primitive cell, too many to list them all here. Only the results shown in Figure 1 and in Figure 2 employ this full structure of uranyl nitrate. The impurity model used to calculate the spectrum in Figure 3 was constructed for a simplified structure: the water molecules were removed and the $UO_2(NO_3)_2$ clusters were placed on a fcc lattice. This higher-symmetry artificial structure accurately represents the environment around the uranium atoms using only 11 atoms in the primitive cell. The LDA band gap of the new structure is noticeably smaller than the gap of the full structure but the unoccupied 5f densities of states of the two structures are almost indistinguishable.

The LDA electronic structure found with the WIEN2K code incorporates scalar-relativistic effects as well as the spin-orbital coupling. The calculations of α-UO_3 were performed with the following parameters: the radii of the muffin-tin spheres were $R_{MT}(U) = 2.20\ a_B$, and $R_{MT}(O) = 1.70\ a_B$, and the basis-set cutoff K_{max} was defined with $R_{MT}(O) \times K_{max} = 7.00$. The calculations of the uranyl nitrate in the full structure employed muffin-tin spheres with radii $R_{MT}(U) = 2.12\ a_B$, $R_{MT}(O) = 1.06\ a_B$, $R_{MT}(N) = 1.11\ a_B$, and $R_{MT}(H) = 0.57\ a_B$, and the basis-set cutoff was given by $R_{MT}(H) \times K_{max} = 2.57$. Finally, for the simplified structure we used $R_{MT}(U) = 2.12\ a_B$, $R_{MT}(O) = 1.16\ a_B$, $R_{MT}(N) = 1.11\ a_B$, and $R_{MT}(N) \times K_{max} = 5.00$. The relatively small muffin-tin spheres around uranium and oxygen atoms in the uranyl nitrate structures are enforced by short U–O and O–H bonds.

RESULTS AND DISCUSSION

Local-density approximation

The simplest approximation to the M_4 absorption spectrum is the density of unoccupied $5f_{5/2}$ states that can be computed using in the density-functional theory (DFT). The densities of states obtained in the local-density approximation are shown in Figure 1. The spectrum of uranyl nitrate is reproduced fairly well, both satellites are present, albeit their intensity is underestimated. The LDA is not quite as successful in UO_3 where only a featureless main line is predicted. There is a faint hint of a shoulder at about 2 eV above the main line that comes from the topmost 5f band that, unlike the

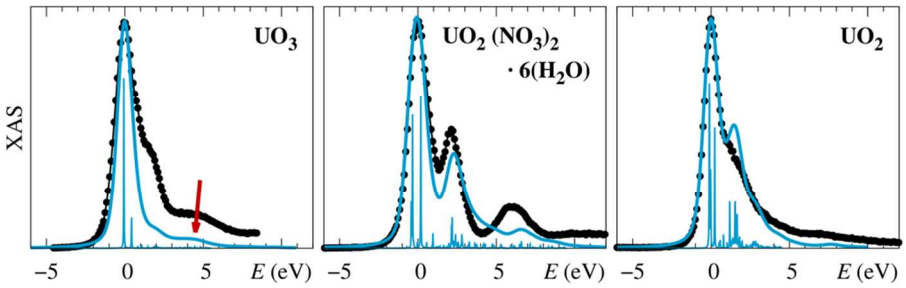

Figure 3. The x-ray absorption spectra calculated in the material-specific impurity model. Apart from the two U^{6+} compounds, the uranium dioxide, where uranium is nominally in the oxidation state U^{4+}, was added for comparison.

other 5f bands, shows some dispersion. It is unlikely, however, that this would be the true origin of the experimentally observed shoulder in UO_3.

The satellites in uranyl nitrate deserve a closer inspection. In Figure 2 we plot LDA densities of states computed with the spin-orbital coupling switched off to make things simpler and more transparent. The uranyl nitrate is compared to a lone $(UO_2)^{2+}$ molecular ion to demonstrate that the satellite features indeed originate in this ion. The environment of the uranium atom is highly anisotropic in this ion and since the molecule is linear, it is a natural choice to project the 5f density of states on the $|l = 3, m\rangle$ basis with quantization axis pointed along the O–U–O bonds. The main line consists of $|m = \pm 2\rangle$ and $|m = \pm 3\rangle$ states that point away from the oxygen atoms (not explicitly shown), and the satellites have $|m = \pm 1\rangle$ and $|m = 0\rangle$ character. Each of these orbitals hybridizes with the oxygen 2p states and forms a bonding combination that is occupied and an antibonding combination that is empty and shows up as a satellite in the absorption spectra. The distance between the bonding and antibonding combinations (about 6 eV for $|m = \pm 1\rangle$ and as much as 9 eV for $|m = 0\rangle$) indicates the hybridization strength between the corresponding 5f and 2p orbitals.

Anderson impurity model

The DFT approximation to the absorption spectra shown in Figure 1 ignores the final state effects induced by the presence of the core hole. These effects are not necessarily small: the impurity-model calculation of the absorption spectrum of uranyl acetylacetonate presented in [9] indicates that a core-hole-induced shake-up tail possibly extends all the way up to the $m = 0$ satellite located 6 eV above the main line. The impurity model used in that study was spherically symmetric and thus it could not correctly reproduce the satellites discussed in the preceding paragraph. Here we present improved impurity-model calculations that combine the core-hole effects with a realistic anisotropic hybridization and crystal field. The results are shown in Figure 3.

In UO_3, the impurity model improves the agreement between the theory and experiment compared to Figure 1. The calculations suggest that the higher-energy shoulder (indicated with an arrow in Figure 3) is a result of the shake-up processes. The shoulder at 2 eV above the main line is not reproduced and it remains a puzzle. In uranyl nitrate, the core-hole effects slightly widen the main line and the shake-up tail overlaps with the satellites that still have their intensity underestimated similarly to the LDA calculation.

In addition to the two U^{6+} compounds, the absorption spectrum of UO_2, a nominally U^{4+} compound, is shown in Figure 3 for comparison. This calculation uses the

impurity model constructed during the LDA+DMFT study reported in [5]. In this case, the shoulder at the high-energy side of the absorption line is identified with a valence $5f^2$ multiplet. The feature remains nearly intact when the impurity model is reduced to a spherically symmetric atomic model by removing the hybridization with the ligand states and the crystal field. The UO_2 calculation is included in order to illustrate that the material-specific impurity model is quite rich: it reproduces valence-band many-body features (UO_2), single-particle features due to anisotropic environment (uranyl nitrate), as well as core-hole-induced shake-up features. Yet, it misses the 2 eV shoulder in UO_3.

CONCLUSIONS

The satellites appearing in the M_4-edge x-ray absorption spectrum of uranyl nitrate are identified with antibonding eigenstates consisting of uranium 5f and oxygen 2p states that are located at the U–O bonds in the $(UO_2)^{2+}$ molecular ion. This finding helps to explain why analogous satellites are observed also in other similar compounds like uranyl acetylacetonate and torbentite, and it provides a quantitative microscopic backing to the mechanism that was suggested on an empirical basis earlier [10,11]. The presented theory offers only partial understanding of the features observed in the absorption spectra of UO_3 and therefore an improved theoretical investigation will need to be performed in the future.

ACKNOWLEDGEMENT

This work was supported by the Czech Science Foundation [grant number 18-02344S]. Access to computing facilities owned by parties and projects contributing to the National Grid Infrastructure MetaCentrum, provided under the program Cesnet LM2015042, is appreciated.

REFERENCES

1. K. Hämäläinen, D. P. Siddons, J. B. Hastings, and L. E. Berman, *Phys. Rev. Lett.* **67**, 2850 (1991).
2. F. de Groot and A. Kotani, *Core Level Spectroscopy of Solids* (CRC Press, Boca Raton, 2008).
3. J. Kolorenč, *Physica B* (2017), DOI: 10.1016/j.physb.2017.08.069
4. K. O. Kvashnina, Y. O. Kvashnin, and S. M. Butorin, *J. Electron. Spectrosc. Relat. Phenom.* **194**, 27 (2014).
5. J. Kolorenč, A. B. Shick, and A. I. Lichtenstein, *Phys. Rev. B* **92**, 085125 (2015).
6. P. Blaha, K. Schwarz, G. K. H. Madsen, D. Kvasnicka, and J. Luitz, *WIEN2K, An Augmented Plane Wave + Local Orbitals Program for Calculating Crystal Properties* (Techn. Universität Wien, Austria, 2001).
7. J. Kuneš, R. Arita, P. Wissgott, A. Toschi, H. Ikeda, and K. Held, *Comput. Phys. Commun.* **181**, 1888 (2010).
8. A. A. Mostofi, J. R. Yates, Y.-S. Lee, I. Souza, D. Vanderbilt, and N. Marzari, *Comput. Phys. Commun.* **178**, 685 (2008).
9. K. O. Kvashnina, S. M. Butorin, P. Martin, and P. Glatzel, *Phys. Rev. Lett.* **111**, 253002 (2013).
10. J. Petiau, G. Calas, D. Petitmaire, A. Bianconi, M. Benfatto, and A. Marcelli, *Phys. Rev. B* **34**, 7350 (1986).
11. S. M. Butorin, *J. Electron. Spectrosc. Relat. Phenom.* **110–111**, 213 (2000).